

## Spin-charge separation in two-component Bose gases

A. Kleine,<sup>1</sup> C. Kollath,<sup>2,3</sup> I. P. McCulloch,<sup>1</sup> T. Giamarchi,<sup>2</sup> and U. Schollwöck<sup>1</sup><sup>1</sup>*Institute for Theoretical Physics C, RWTH Aachen, D-52056 Aachen, Germany*<sup>2</sup>*DPMC-MaNEP, University of Geneva, 24 Quai Ernest-Ansermet, CH-1211 Geneva, Switzerland*<sup>3</sup>*Centre de Physique Théorique, Ecole Polytechnique, 91128 Palaiseau Cedex, France*

(Received 5 June 2007; published 9 January 2008)

We show that one of the key characteristics of interacting one-dimensional electronic quantum systems, the separation of spin and charge, can be observed in a two-component system of bosonic ultracold atoms even close to a competing phase separation regime. To this purpose we determine the real-time evolution of a single particle excitation and the single particle spectral function using density-matrix renormalization group techniques. Due to efficient bosonic cooling and good tunability this setup exhibits very good conditions for observing this strong correlation effect. In anticipation of experimental realizations we calculate the velocities for spin and charge perturbations for a wide range of parameters.

DOI: [10.1103/PhysRevA.77.013607](https://doi.org/10.1103/PhysRevA.77.013607)

PACS number(s): 03.75.Mn, 03.75.Kk, 05.30.Jp, 71.10.Pm

### I. INTRODUCTION

One of the most exciting recent events is the ever-growing interplay between previously disconnected fields of physics, such as quantum optics and condensed matter physics. In particular, cold atomic systems have opened the way to engineer strongly interacting quantum many-body systems of unique purity. The unprecedented control over interaction strength and dimensionality allows the realization of “quantum simulators” where fundamental but hard to analyze phenomena in strongly correlated systems could be observed and controlled. Examples are the observation of superfluid to Mott insulator transition for Bose gases [1] and the fermionization of strongly interacting one-dimensional bosons [2,3].

Among interacting systems, the physics depends very strongly on the dimensionality. In one-dimensional systems the interactions play a major role and lead to drastically different physics than for their higher dimensional counterpart. Typically, interactions in one-dimensional systems lead to a Luttinger liquid state where the excitations of the system are collective excitations [4]. The importance of such a state for a large variety of experimental devices in condensed matter has led to a hunt to observe its properties. A remarkable consequence of such a state is the absence of single particle excitations. This means that a quantum particle that would normally carry both charge and spin degrees of freedom fractionalizes into two different collective excitations, a spin and a charge excitation. Such a fractionalization of a single particle excitation is the hallmark of collective effects caused by interactions. However, just as detecting fractional excitations in the case of the quantum Hall effect is difficult [5], observing spin-charge separation has proven elusive despite several experimental attempts [6–8]. So far, the best experimental evidence is provided by tunneling between quantum wires where interference effects are due to the existence of two different velocities [9]. However, in these systems it is hard to quantify or to tune the interaction between the particles which causes the collective effects. Since control of the interaction is a routing procedure in ultracold gases, the possible realization of the phenomenon of spin-charge separation has also been discussed in the context of cold fermionic

gases [10–13] and strongly interacting bosonic gases [14].

However, proposals to observe spin-charge separation in ultracold fermionic gases are still plagued by the currently quite high temperatures in such systems. A much better setup to test for spin-charge separation would be two-component Bose gases, for example, using the  $|F=2, m_F=-1\rangle$  and the  $|F=1, m_F=1\rangle$  hyperfine states of  $^{87}\text{Rb}$  [15,16]. Experimentally, this system retains the advantages of the fermionic ultracold atom setup while allowing for much lower temperatures due to the more efficient cooling techniques available for bosons. Theoretical studies [17,18] for one-dimensional systems predict that close to the experimentally accessible parameter regime of almost equal interspecies and intraspecies interaction strength phase separation occurs. This is the remaining potential experimental complication in the setup.

In this work we demonstrate the phenomenon of spin-charge separation in the experimentally relevant parameter regime, allowing us to use this system to unambiguously test for spin-charge separation. We hereby consider a system of one-dimensional tubes with an additional optical lattice potential applied along the tube directions. We calculate both the real-time evolution of a single particle excitation and the dynamical single particle spectral function of the two-component bosonic systems. We show that both these quantities demonstrate the separation of a single particle excitation into spin and charge. We further determine the velocity of spin and charge for experimentally relevant parameter regimes. To perform the calculations we use variants of the density-matrix renormalization group method (DMRG) [19,20]. The numerical treatment is necessary to obtain reliable predictions for experimental realizations, due to the close proximity of this regime to phase separation.

### II. MODELING SPIN-CHARGE SEPARATION IN TWO-COMPONENT BOSONIC SYSTEMS

A one-dimensional two-component Bose gas in an optical lattice [21] can be described by the two-component Bose-Hubbard model

$$H = -J \sum_{j,\nu} (b_{j+1,\nu}^\dagger b_{j,\nu} + \text{H.c.}) + \sum_{j,\nu} \frac{U_\nu \hat{n}_{j,\nu} (\hat{n}_{j,\nu} - 1)}{2} + U_{12} \sum_j \hat{n}_{j,1} \hat{n}_{j,2} + \sum_{j,\nu} \varepsilon_{j,\nu} \hat{n}_{j,\nu}. \quad (1)$$

Here  $j$  is the site index and  $\nu=1,2$  labels the two different hyperfine states of the system,  $b$  and  $b^\dagger$  are the annihilation and creation operators and  $\hat{n}$  is the number operator. The first term models the kinetic energy of the atoms. The intraspecies interaction is described by the  $U_\nu$  term. We use  $U:=U_1=U_2$  as it is approximately realized for commonly used hyperfine states of  $^{87}\text{Rb}$  [22] if not mentioned otherwise. The interspecies interaction is given by the  $U_{12}$  term and the last term describes external potentials. In the following we use the dimensionless parameters  $u=U/J$  and  $u_{12}=U_{12}/J$ . We define the charge density  $n_{j,c}=n_{j,1}+n_{j,2}$  and the spin density  $n_{j,s}=n_{j,1}-n_{j,2}$ . We focus on systems with an average filling  $n=\sum_j n_{j,1}/L=\sum_j n_{j,2}/L$  smaller than one particle per site and parameter regimes of not too large values of  $u_{12}$  for which the system does not undergo a phase separation. Indeed if  $u_{12}$  becomes too large one can expect phase separation since the spin exchange between the two spin species becomes dominantly ferromagnetic. In our finite size systems, we numerically do observe this tendency to phase separate, as indicated by a much slower convergence of our numerics. The boundary corresponds to  $u_{12} \approx u$  [18]. In the above expressions,  $L$  is the number of sites in the system and  $a$  is the lattice spacing. We use if not stated otherwise  $\hbar=1$ ,  $J=1$ , and  $a=1$ . If the perpendicular oscillator length of the system is larger than the 3D scattering length, the connection between the experimental parameters, the optical lattice depth and the scattering lengths, to the theoretical parameters of the Bose-Hubbard model can be made using the tight binding approximation [21].

In the superfluid phase for low interaction strength or more precisely if the dimensionless parameter  $\gamma=u/(2n_c) < 1$  and  $\gamma_{12}=u_{12}/(2n_c) < 1$  are small, the Bose-Hubbard model can directly be mapped onto a continuous model by taking  $Ja^2=\text{const}$  and  $a \rightarrow 0$ . In this limit the Bose-Hubbard model becomes equivalent to the Lieb-Liniger model [23,24]. The Hamiltonian for two bosonic species is

$$H_{\text{LL}} = \int dx \sum_{\nu=1,2} \left( \frac{1}{2M} |\partial_x \Psi_\nu(x)|^2 + V(x) \Psi_\nu^\dagger(x) \Psi_\nu(x) + \frac{g}{2} [\Psi_\nu^\dagger(x)]^2 [\Psi_\nu(x)]^2 \right) + \frac{g_{12}}{2} \int dx [\Psi_1^\dagger(x) \Psi_1(x)] [\Psi_2^\dagger(x) \Psi_2(x)]. \quad (2)$$

Here  $\Psi^{(\dagger)}$  is the bosonic annihilation (creation) operator,  $V$  is the external potential, and  $g$  and  $g_{12}$  are the strengths of the intraspecies and interspecies interaction, respectively. In this limit, the hopping parameter of the lattice model is related to the mass  $M$  of the atoms by  $Ja^2=\frac{1}{2M}$ , the interaction strength to the  $\delta$ -interaction strength by  $Ua=g$  and  $U_{12}a=g_{12}$ , and the density  $\rho$  to the filling factor  $n$  by  $\rho a=n$ . A discussion of the validity of this mapping for one-component gas focusing on

the value of the sound velocity is presented in Ref. [25]. In the hydrodynamic approximation [26] the sound velocities of this model are given by

$$v_{c,s} = v_0 \sqrt{1 \pm g_{12}/g}, \quad (3)$$

with

$$v_0 = \sqrt{g\rho/M}. \quad (4)$$

As in the case of a single component gas this expression for the velocity is only valid for low values of  $\gamma_c=Mg/\rho$  [25]. For the special case  $g_{12}=g$  the sound velocity has been determined using the Bethe ansatz [27,28].

In a superfluid phase away from the transition to phase separation the low energy physics can be approximated by a density-phase representation of the bosons as used in the bosonization method [4,29]. The description of the low energy properties of the Bose-Hubbard model by the bosonization approach is valid for a wider parameter regime than the continuum limit equation (2). In particular it does not rely on the low-filling limit as the continuum limit equation (2). The bosonization description is a density-phase representation of the bosons [4,29], i.e., the density is expressed as  $\rho_\nu(x) \approx (\rho_0 - \frac{1}{\pi} \partial_x \phi_\nu) \sum_{m=-\infty}^{\infty} \exp^{2im[\phi_\nu(x) + \pi\rho_0 x]}$  and the single boson operator as  $\Psi_\nu(x) \propto \exp^{i\theta_\nu(x)} \rho_\nu(x)^{1/2}$ , where  $\rho_0$  is the average density, and  $\frac{1}{\pi} \partial_x \phi_\nu$  and  $\theta_\nu$  are conjugate operators.

In this representation the Hamiltonian of the two-component Bose gas is totally separated into one part for the charge and one part for the spin degrees of freedom [30],

$$H = H_c + H_s \quad (5)$$

with

$$H_c = \frac{1}{2\pi} \int dx \left( v_c K_c (\partial \theta_c)^2 + \frac{v_c}{K_c} (\partial_x \phi_c)^2 \right) \quad (6)$$

and

$$H_s = \frac{1}{2\pi} \int dx \left( v_s K_s (\partial \theta_s)^2 + \frac{v_s}{K_s} (\partial_x \phi_s)^2 \right) + \frac{g_{12}}{(\pi\rho^{-1})^2} \int dx \cos(\sqrt{8}\phi_s). \quad (7)$$

The physics is fully determined by the velocities  $v_{c,s}$  and the so-called Luttinger parameters  $K_{c,s}$  for spin ( $s$ ) and charge ( $c$ ). Therefore, the separation of a single particle excitation into spin and charge excitations is expected. Note that the phenomenon of a complete decoupling merely requires the presence of two flavors of particles; the SU(2) symmetry of electronic spin is not necessary. In fact, expressing real spin via two flavors of Schwinger bosons matches our identification, except that for full SU(2) symmetry a local constraint  $n_{j,1}+n_{j,2}=1$  would have to be enforced, corresponding to diverging interspecies and intraspecies particle repulsion at density 1. The parameters of two interacting species of bosons can be related to the parameters  $K$  and  $v_0$  for the single species case [30] by

$$v_{c,s} = v_0 \sqrt{1 \pm (g_{12}K)/(\pi v_0)} \quad (8)$$

and

$$K_{c,s} = K/\sqrt{1 \pm (g_{12}K)/(\pi v_0)}.$$

In the limit of small interactions, the single species parameters  $K$  and  $v_0$  can be directly related to the Lieb-Liniger model and to the Bose-Hubbard Hamiltonian equation (1) [4]. In this regime the expressions of the sound velocity of the continuum description are recovered. For higher values of the interaction strength if one assumes bosonization to be justified, the relation of the parameters of the Bose-Hubbard model to the universal parameters  $K$  and  $v_0$  even for the single species situation is unknown. This relation must be determined numerically [25]. For a two-component mixture with large values of the interspecies interaction of the order of the intraspecies interaction—which is the experimentally relevant case—the system approaches the transition to phase separation. In the regime of phase separation the bosonization approach breaks down.

### III. EVIDENCE OF SPIN-CHARGE SEPARATION

Snapshots of the real time evolution of a single particle excitation in a two-component bosonic system are shown in Fig. 1. The single particle excitation at time  $t=0$  is prepared by the application of the creation operator of one species, say 1, on site  $L/2$  to the ground state  $|\psi_0\rangle$ , i.e.,  $b_{L/2,1}^\dagger|\psi_0\rangle$ . The resulting sharp peaks in the density distributions are shown in Fig. 1(a). For  $t>0$  the time evolution of the single particle excitation is calculated using the adaptive time-dependent DMRG [31,32]. The time-evolution is performed using a Krylov algorithm [33] in a matrix product state basis with a fixed error bound for each time step of the order of  $\|\Psi(t+\Delta t) - \exp(-iH\Delta t)|\Psi(t)\rangle\|^2 < 10^{-5}$ . The step size  $\Delta t = 0.2\hbar/J$  and 6 to 10 Krylov vectors were used resulting in Hilbert spaces with a local dimension of a few thousand states. As can be seen in the snapshots in Fig. 1 the initial single particle excitation splits up into two counterpropagating density waves. Due to their different spin and charge velocities, after a period of time a clear separation of the density waves is seen [cf. Fig. 1(c)] [47]. Note that the chosen parameters correspond to an experimentally relevant situation of a mixture of  $^{87}\text{Rb}$  using the  $|F=2, m_F=-1\rangle$  and the  $|F=1, m_F=1\rangle$  hyperfine states adjusting the scattering length to  $a_{12}=80a_B$  (for more details see discussion on experimental parameters).

Additionally to the time evolution of a single particle excitation, we obtained the single particle spectral function  $A(q, \omega) = \frac{1}{\pi} \text{Im} \langle b_{q,1} \frac{1}{H - \omega - i\eta - E_0} b_{q,1}^\dagger \rangle$  as shown in Fig. 2. For fermions this function is known to exhibit two peaks at the spin and charge excitation energies [34,35], showing a direct signature of the spin-charge separation. For the bosons computing this spectral function is more involved and up to very recently it was only derived for a single-component bosonic system [36–38]. An expression for the correlation functions which allows us to obtain the single particle correlation function within the bosonization treatment for a two-component bosonic system was derived in [39]. Power law singularities

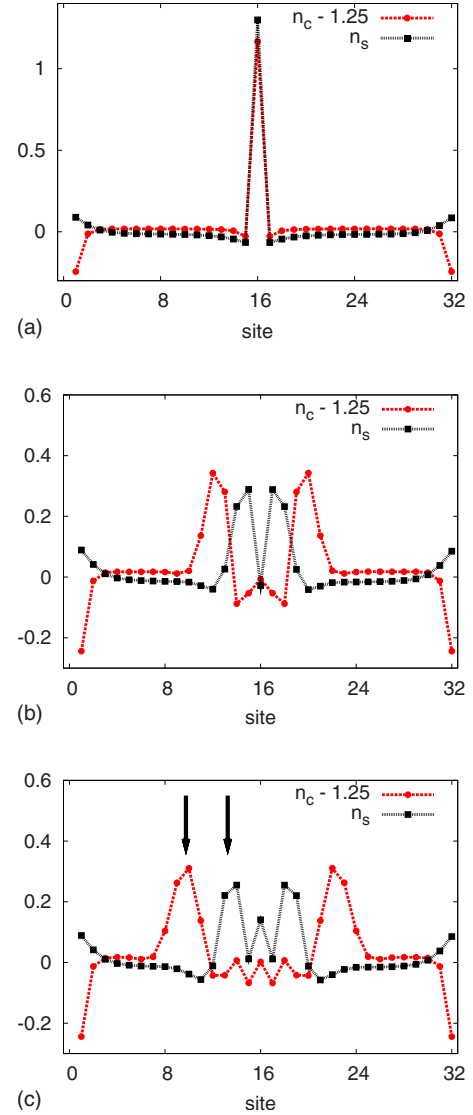


FIG. 1. (Color online) Snapshots of the time evolution of the charge- and spin-density distribution of a single particle excitation created at time  $t=0\hbar/J$ : (a) at time  $t=0\hbar/J$ , (b) at time  $t=1.5\hbar/J$ , and (c) at time  $t=2.5\hbar/J$ . The system parameters are  $n_{1,2}=0.625$ ,  $U_1/J=2.983$ ,  $U_2/J=2.712$ ,  $U_{12}/J=2.377$ . The charge density is shifted by 1.25 for better visibility. The arrows in (c) mark the clear separation of the charge- and the spin-density waves.

at  $qv_{c,s}$  are obtained with respective exponents  $1/4K_{c,s} + 1/2K_{s,c} - 1$ . For the values of the Luttinger parameters (as shown in Fig. 2) one thus expects two divergent peaks. We show in Fig. 2 the full spectral function for our microscopic model, as calculated numerically using a matrix product state generalization of the correction vector method [37,40]. Our results show clearly the appearance of the two separated peaks, the lower representing the spin and the upper the charge excitation branch. The positions are close to the predicted values  $v_{c,s}q$  of bosonization results. The discrepancy can be attributed to the band curvature that exists in the microscopic model and which in the bosonization is taken to be a strictly linear dispersion relation. Thus, both the real time evolution of a single particle function and the single

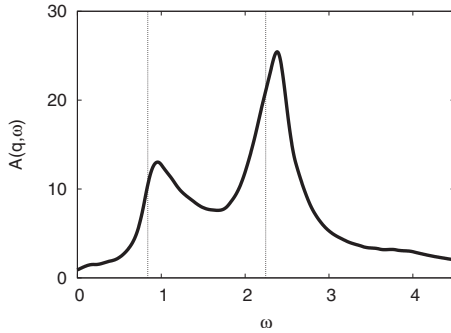


FIG. 2. One-particle spectral function at momentum  $q = 20/65\pi/a$ . Two peaks corresponding to the spin and the charge excitations can be distinguished. The vertical lines mark the position of  $v_{c,s}q$ . The following parameters were used:  $n=0.625$ ,  $u=3$ ,  $u_{12}=2.1$  on a system with  $L=64$  sites and a broadening  $\eta=0.1$ . Restoring the units, the  $x$  axis is  $J/\hbar$ .

particle spectral function show clear signatures of separation of spin and charge.

#### IV. DETERMINATION OF THE SPIN AND CHARGE VELOCITIES

To observe the separation of spin and charge excitations experimentally in a system of ultracold bosons, knowledge of the spin and charge velocities is indispensable. This is since currently spectral functions are not accessible, merely a direct observation of the evolution of density perturbations. As the spatial range of the experimental setups is small, a substantial difference in velocities is required to observe an effect on the available length scales. We therefore determined the velocities for a wide range of parameters. This was done calculating the time evolution of a small spin- and charge-density perturbation, respectively. The density perturbation was created at time  $t=0$  applying an external potential of Gaussian form  $\varepsilon_{\nu,j} = \varepsilon_0 \exp\left(-\frac{(j-j_0)^2}{2\sigma_j^2}\right)$ , where  $\nu=c,s$ . At time  $t=0$  the potential is switched off and the time evolution of the density perturbation is calculated. The errors in the obtained velocities are of the order of  $0.01aJ/\hbar$  for small  $u_{12}$  and increase with larger  $u_{12}$ .

In Fig. 3 we show the dependence of the velocities on the interspecies interaction for two different values of the parameter  $\gamma$ . For both parameter regimes, the charge velocity increases with increasing interaction whereas the spin velocity decreases. Therefore as  $u_{12}$  increases, the difference between the charge and the spin velocities becomes larger. For a vanishing interspecies interaction it was shown in Ref. [25] that for  $\gamma < 1$  the bosonization and the solution of the exactly solvable Lieb-Liniger model agree approximately with the velocities in the Bose-Hubbard model. In Fig. 3(a) we find for  $\gamma \approx 1.1$  very good agreement with the analytical solutions up to interspecies interaction strength  $u_{12} \lesssim 1.5$ . For  $\gamma \approx 2.4$  [cf. Fig. 3(b)] even for vanishing interspecies interaction the deviations from the direct relation between the parameters in the Bose-Hubbard model are considerable (cf. [25]). However, we find that the dependence of the velocities on the

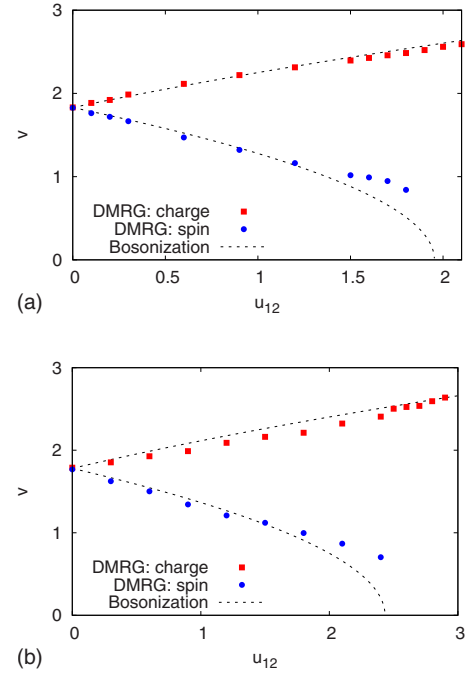


FIG. 3. (Color online) Dependence of the charge and spin velocities on the interspecies interaction strength for (a)  $u=2$  and  $n \approx 0.88$  and (b)  $u=3$  and  $n \approx 0.63$ . A comparison of analytical results (line, see text) and numerical DMRG results (symbols) is shown. Restoring the units of the velocities, they are measured in units  $aJ/\hbar$ . Note that the errors of the DMRG results increase close to  $u_{12} \approx u$ .

interspecies interaction strength via Eq. (8) is still a good approximation up to  $u_{12} \approx 1.5$  correcting by the numerically determined value for  $v_0$  and  $K$ . As is obvious from Fig. 3 for larger values  $u_{12} \lesssim u$  the results for the spin velocity start to deviate for both values of  $\gamma$  from the perturbative relation (8). Our numerical results provide an accurate determination of the velocities in this regime, hard to access analytically, since the perturbative expression (8) becomes inaccurate. If the intraspecies interaction  $u_{12}$  becomes too large, the spin velocity ultimately goes to zero. The spin excitations are characterized around that point by strong damping and strong diffusion, and we cannot numerically compute their exact velocity close to phase transition. This phase transition corresponds to a dominantly ferromagnetic ground state and thus to phase separation. The dispersion of the spin excitations beyond the phase transition point is not longer linear but becomes parabolic [27]. The physics in this regime is thus radically different [46] from the one of a Luttinger liquid with linear modes and requires a totally different analysis. In order to test for the spin-charge separation in a Luttinger liquid, it is thus important to stay below this point, but at the same time to have a large velocity difference to make the observation easier. In that perspective an optimal regime to test for the spin-charge separation and make a quantitative comparison with our numerical results is around  $u_{12} = 2/3u$ , where our numerical results can provide qualitatively accurate results for the velocities for comparison with the experimentally measured ones.

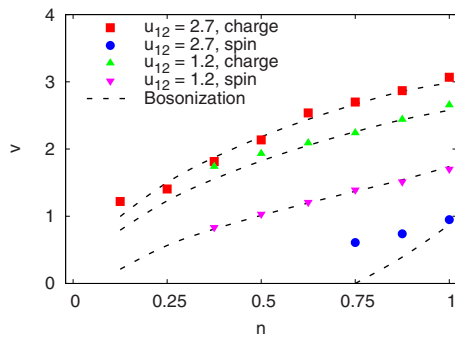


FIG. 4. (Color online) Dependence of the charge and spin velocities on the charge background density. A comparison of analytical results (lines, see text) and numerical DMRG results (symbols) is shown. The parameters used are (a)  $u=3$ ,  $u_{12}=1.2$  and (b)  $u=3$ ,  $u_{12}=2.7$ . Restoring the units of the velocities, they are measured in units  $aJ/\hbar$ .

In Fig. 4 we show for two different fixed interspecies interaction strengths the dependence of the velocities on the density. The charge and the spin velocities rise with increasing background charge density. (Note, even at  $n_c=1$  the system is in the superfluid regime.) The increase of the velocities is described to good accuracy using the perturbative form (8), provided we use numerically obtained values of  $K$  and  $v_0$ . For large  $u_{12}$  and small  $n_c$  the results for the velocities from DMRG, in particular the spin velocity, deviate considerably from Eq. (8), showing that the approximate relation cannot be used in this regime. Our finding of the dependencies can be used to predict the velocities for experimentally interesting parameter regimes.

## V. EXPERIMENTAL REALIZATION

In recent experiments for the preparation of a mixture of two bosonic components in optical lattices mostly two hyperfine states of  $^{87}\text{Rb}$  are used, e.g., the  $|F=2, m_F=-1\rangle$  and the  $|F=1, m_F=1\rangle$  hyperfine states. The intraspecies scattering lengths are  $a_2=91.28a_B$  and  $a_1=100.4a_B$  [22], respectively, where  $a_B$  is the Bohr radius. For these states the interspecies

scattering length is of the same order of magnitude as the intraspecies scattering length and can be tuned about 20% using a Feshbach resonance [16,15]. Thereby the experimental parameters are close to the competing phase separation regime. These mixtures can be confined to one-dimensional structures using strongly anisotropic lattices [2,3,41,42]. The experimental parameters in such a system are related to the parameters of the two-component Bose-Hubbard model. For example, in Fig. 1 we used the parameters corresponding to the experimental situation with scattering length  $a_{12}=80a_B$  and a lattice height of  $V_0=4.3E_r$ . The most intuitive observation of the phenomenon of spin-charge separation in these systems is to generate a single particle excitation and then follow the evolution of the excitation in real time. This can be done measuring the spin-resolved density over a certain region. The creation of a single particle excitation can be done, e.g., using out coupling of single particles by the application of a magnetic field gradient for addressability and a microwave field [43–45]. The magnetic field gradient can be applied since the two hyperfine states have approximately the same magnetic moment. The efficiency of such a technique for generating single particle excitations was demonstrated [44] using a cavity. The microwave field could be chosen to couple the  $|F=1, m_F=1\rangle$  hyperfine state to, e.g., the  $|F=2, m_F=2\rangle$ . This has the advantage that scattering with the  $|F=1, m_F=1\rangle$  state is suppressed. The measurement of the density resolved over a region of approximately 10 lattice sites can then be performed using again the magnetic field gradient to get an unambiguous signal.

## ACKNOWLEDGMENTS

The authors would like to thank J. S. Caux, S. Fölling, M. Köhl, and B. Paredes for fruitful discussions. Two of the authors (A.K., U.S.) acknowledge support by the DFG (Contract No. FOR 801) and two of the authors (C.K., T.G.) by the Swiss National Science Foundation under MaNEP and Division II and the CNRS. One of the authors (C.K.) thanks the Institut Henri Poincaré-Centre Emile Borel for its hospitality and the RTRA network Triangle de la Physique for support during the final part of the work.

- 
- [1] M. Greiner, O. Mandel, T. Esslinger, T. W. Hänsch, and I. Bloch, *Nature (London)* **415**, 39 (2002).
  - [2] B. Paredes, A. Widera, V. Murg, O. Mandel, S. Fölling, I. Cirac, G. V. Shlyapnikov, T. W. Hänsch, and I. Bloch, *Nature (London)* **429**, 277 (2004).
  - [3] T. Kinoshita, T. Wenger, and D. S. Weiss, *Science* **305**, 1125 (2004).
  - [4] T. Giamarchi, *Quantum Physics in One Dimension* (Oxford University Press, Oxford, 2004).
  - [5] C. Glattli, in *High Magnetic Fields: Applications in Condensed Matter Physics and Spectroscopy*, edited by C. Berthier *et al.* (Springer-Verlag, Berlin, 2002), p. 1.
  - [6] P. Segovia, D. Purdie, M. Hengsberger, and Y. Baer, *Nature (London)* **402**, 504 (1999).
  - [7] T. Lorenz, M. Hofmann, M. Grüninger, A. Freimuth, G. S. Uhrig, M. Dumm, and M. Dressel, *Nature (London)* **418**, 614 (2002).
  - [8] C. Kim, A. Y. Matsuura, Z. X. Shen, N. Motoyama, H. Eisaki, S. Uchida, T. Tohyama, and S. Maekawa, *Phys. Rev. Lett.* **77**, 4054 (1996).
  - [9] O. M. Auslaender, H. Steinberg, A. Yacoby, Y. Tserkovnyak, B. I. Halperin, K. W. Baldwin, L. N. Pfeiffer, and K. W. West, *Science* **308**, 88 (2005).
  - [10] A. Recati, P. O. Fedichev, W. Zwerger, and P. Zoller, *Phys. Rev. Lett.* **90**, 020401 (2003).
  - [11] L. Kecke, H. Grabert, and W. Hausler, *Phys. Rev. Lett.* **94**, 176802 (2005).
  - [12] C. Kollath, U. Schollwöck, and W. Zwerger, *Phys. Rev. Lett.*

- 95**, 176401 (2005).
- [13] C. Kollath and U. Schollwöck, *New J. Phys.* **8**, 220 (2006).
- [14] B. Paredes and J. I. Cirac, *Phys. Rev. Lett.* **90**, 150402 (2003).
- [15] M. Erhard, H. Schmaljohann, J. Kronjäger, K. Bongs, and K. Sengstock, *Phys. Rev. A* **69**, 032705 (2004).
- [16] A. Widera, O. Mandel, M. Greiner, S. Kreim, T. W. Hänsch, and I. Bloch, *Phys. Rev. Lett.* **92**, 160406 (2004).
- [17] M. A. Cazalilla and A. F. Ho, *Phys. Rev. Lett.* **91**, 150403 (2003).
- [18] T. Mishra, R. V. Pai, and B. P. Das, *Phys. Rev. A* **76**, 013604 (2007).
- [19] S. R. White, *Phys. Rev. Lett.* **69**, 2863 (1992).
- [20] U. Schollwöck, *Rev. Mod. Phys.* **77**, 259 (2005).
- [21] D. Jaksch, C. Bruder, J. I. Cirac, C. W. Gardiner, and P. Zoller, *Phys. Rev. Lett.* **81**, 3108 (1998).
- [22] A. Widera, F. Gerbier, S. Foelling, T. Gericke, O. Mandel, and I. Bloch, *New J. Phys.* **8**, 152 (2006).
- [23] E. H. Lieb and W. Liniger, *Phys. Rev.* **130**, 1605 (1963).
- [24] E. H. Lieb, *Phys. Rev.* **130**, 1616 (1963).
- [25] C. Kollath, U. Schollwöck, J. von Delft, and W. Zwerger, *Phys. Rev. A* **71**, 053606 (2005).
- [26] L. Pitaevskii and S. Stringari, *Bose-Einstein Condensation* (Oxford University Press, Oxford, 2003).
- [27] J. N. Fuchs, D. M. Gangardt, T. Keilmann, and G. V. Shlyapnikov, *Phys. Rev. Lett.* **95**, 150402 (2005).
- [28] M. T. Batchelor, M. Bortz, X. W. Guan, and N. Oelkers, *J. Stat. Mech.* (2006) P03016.
- [29] F. D. M. Haldane, *Phys. Rev. Lett.* **47**, 1840 (1981).
- [30] E. Orignac and T. Giamarchi, *Phys. Rev. B* **57**, 11713 (1998).
- [31] A. J. Daley, C. Kollath, U. Schollwöck, and G. Vidal, *J. Stat. Mech.* (2004) P04005.
- [32] S. R. White and A. E. Feiguin, *Phys. Rev. Lett.* **93**, 076401 (2004).
- [33] M. Hochbruck and C. Lubich, *SIAM J. Numer. Anal.* **34**, 1911 (1997).
- [34] V. Meden and K. Schönhammer, *Phys. Rev. B* **46**, 15753 (1992).
- [35] J. Voit, *Phys. Rev. B* **47**, 6740 (1993).
- [36] F. D. M. Haldane, *Phys. Rev. Lett.* **47**, 1840 (1981).
- [37] T. D. Kühner and S. R. White, *Phys. Rev. B* **60**, 335 (1999).
- [38] J.-S. Caux and P. Calabrese, *Phys. Rev. A* **74**, 031605 (2006).
- [39] A. Iucci, G. A. Fiete, and T. Giamarchi, *Phys. Rev. B* **75**, 205116 (2007).
- [40] A. Friedrich, A. K. Kolezhuk, I. P. McCulloch, and U. Schollwöck, *Phys. Rev. B* **75**, 094414 (2007).
- [41] H. Moritz, T. Stöferle, M. Kohl, and T. Esslinger, *Phys. Rev. Lett.* **91**, 250402 (2003).
- [42] B. Laburthe Tolra, K. M. O'Hara, J. H. Huckans, W. D. Phillips, S. L. Rolston, and J. V. Porto, *Phys. Rev. Lett.* **92**, 190401 (2004).
- [43] I. Bloch, T. Hänsch, and T. Esslinger, *Nature (London)* **403**, 166 (2000).
- [44] A. Öttl, S. Ritter, M. Köhl, and T. Esslinger, *Phys. Rev. Lett.* **95**, 090404 (2005).
- [45] S. Fölling, A. Widera, T. Müller, F. Gerbier, and I. Bloch, *Phys. Rev. Lett.* **97**, 060403 (2006).
- [46] M. Zvonarev, V. Cheianov, and T. Giamarchi, e-print arXiv:0708.3638v1.
- [47] The remaining interaction between the spin and the charge degrees of freedom for short times can cause small additional structures beside the main peaks in the density wave profiles [Fig. 1(c)].